AGU Fall Meeting 2019 SA21B-3103

An Exospheric Temperature Model Using a Polyhedral Grid

Daniel R. Weimer[1,2], Piyush M. Mehta[3], W. Kent Tobiska[4],
Martin G. Mlynczak[5], and Linda A. Hunt[6]

[1]Center for Space Science and Engineering Research, Virginia Tech, Blacksburg, VA
[2]National Institute of Aerospace, Hampton, VA
[3]Statler College of Engineering and Mineral Resources, West Virginia Univ., Morgantown, WV
[4]Space Environment Technologies, Los Angeles, CA
[5]Science Directorate, NASA Langley Research Center, Hampton, VA
[6]Science Systems and Applications, Inc., Hampton, VA

Introduction

A high-resolution model of exospheric temperatures has been developed, with the objective of predicting the global mapping of exospheric temperatures with greater accuracy. These temperatures can be used to predict the neutral densities, when substituted into the calculations used by the NRLMSISE-00 model [*Picone et al,* 2002]. The new model is based on measurements of the neutral densities with the CHAMP, GRACE, and Swarm satellites (A&B).

Method

1. Using the NRLMSISE-00 model, exospheric temperatures are found that produced densities matching the measured values [*Weimer et al*, 2016].

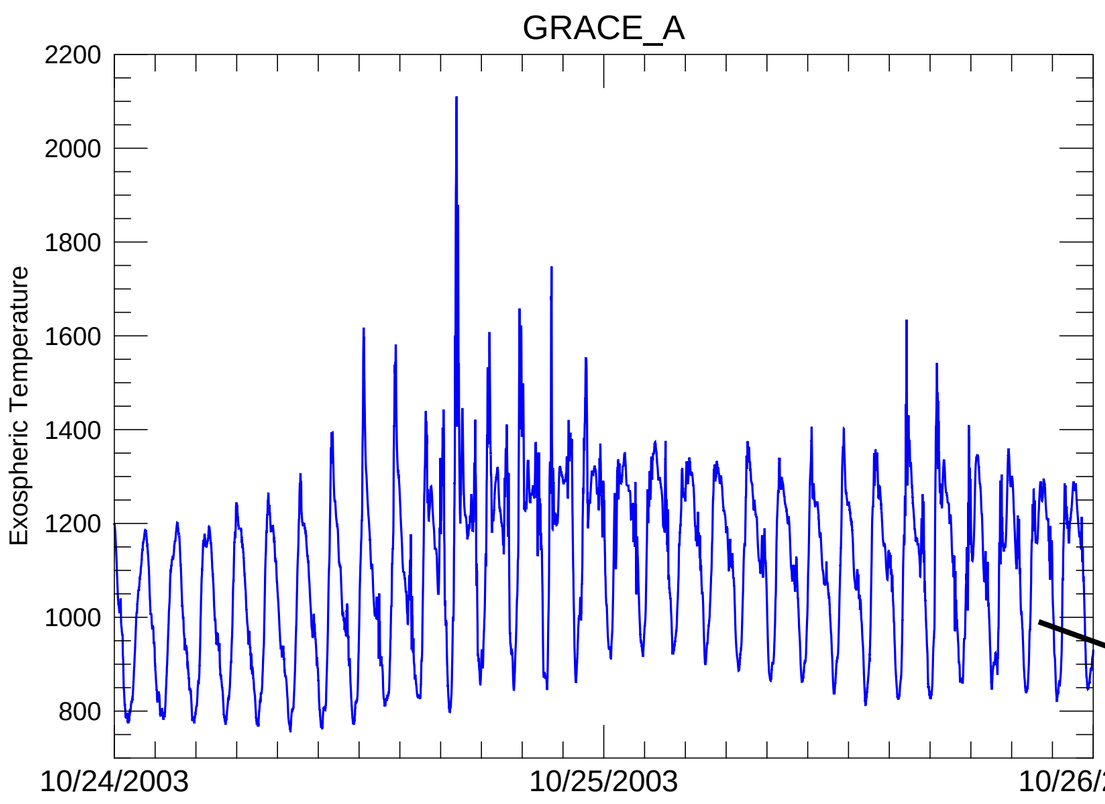

2. Using orbit positions in latitude/solar local time, sort these temperature values by location on a polyhedral grid.

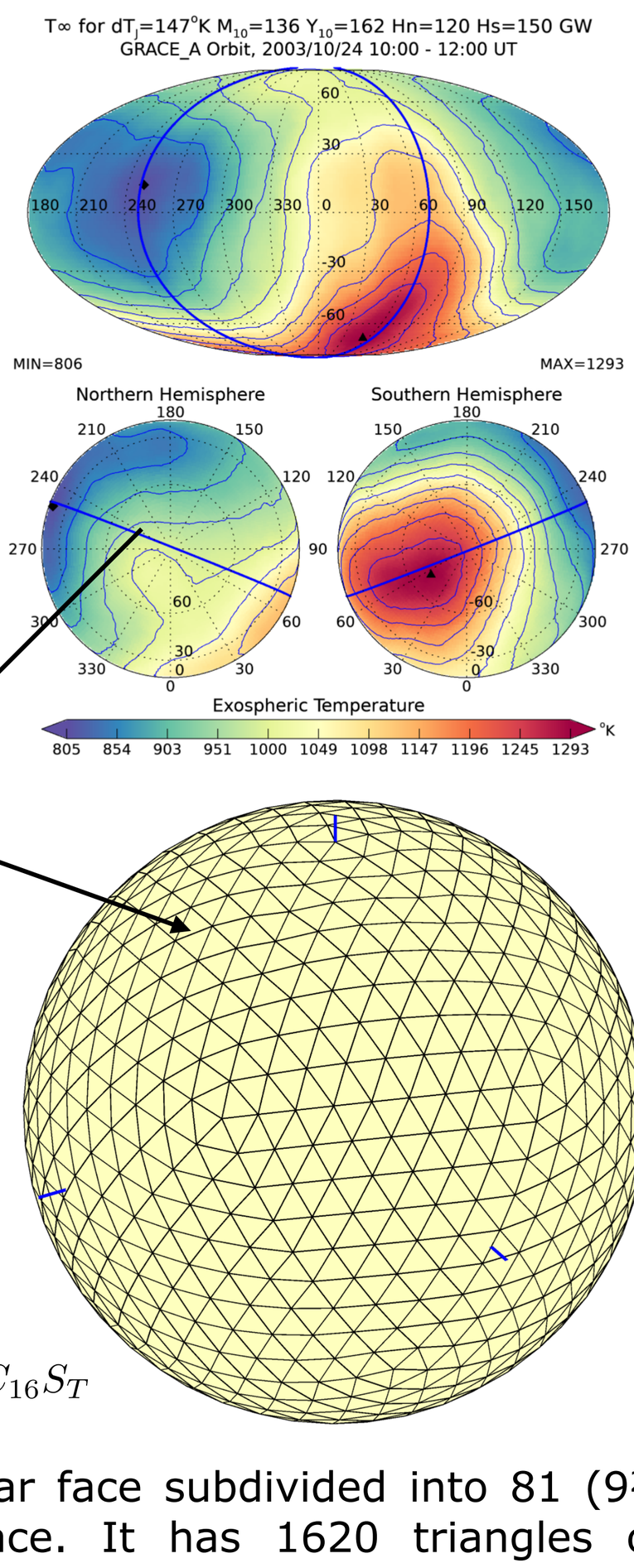

3. The temperature data in each grid cell, along with their associated dates, times, and other information, are used in a least-error fit to derive a set of coefficients that are associated with each of the 1620 cells:

$$
\begin{aligned}
T\infty = \; & C_0 + C_1\Delta T + C_2 S_{10} + C_3\sqrt{M_{10}} + \\
& C_4\Delta T\sin(\theta_D) + C_5\Delta T\cos(\theta_D) + C_6 S_{10}\sin(\theta_D) + C_7 S_{10}\cos(\theta_D) + \\
& C_8\sqrt{M_{10}}\sin(\theta_D) + C_9\sqrt{M_{10}}\cos(\theta_D) + C_{10}\sin(2\theta_D) + C_{11}\cos(2\theta_D) + \\
& C_{12}\sin(\phi_{UT}) + C_{13}\cos(\phi_{UT}) + C_{14} S_T\sin(\phi_{UT}) + C_{15} S_T\cos(\phi_{UT}) + C_{16} S_T
\end{aligned}
$$

The grid is from a 20-sided icosahedron, with each triangular face subdivided into 81 (9^2) equilateral triangles that are projected to a spherical surface. It has 1620 triangles of approximately equal area. The blue lines in the figure show three orthogonal axes, with one pole at the top. The edges of the triangles span approximately 7°. For convenience the new model is referred to with the acronym EXTEMPLAR (EXospheric TEMperatures on a PoLyhedrAl gRid).

Multiple, incremental versions of the model functions have been tested during development. The lowest residual errors are produced with the formula shown above. C_0 — C_{16} are the regression coefficients. S_{10} and M_{10} are solar indices defined by *Tobiska et al.* [2008]. The parameter ΔT is the global change in the exospheric temperature as a function of time that is calculated from a differential equation in which the temperature increases in proportion to the total W05 Poynting flux [*Weimer,* 2005a, 2005b], and decreases at an exponential, cooling rate. [*Weimer et al.,* 2011; 2015]. In one version of the model the cooling is rate is determined by the total power of nitric oxide emissions, as measured with the SABER instrument on the TIMED satellite. In another version the cooling rate is an exponential function of the the exospheric temperature multiplied with a model equation for the level of nitric oxide. The parameter θ_{DOY} is the angular representation of the day-of-year, while ϕ_{UT} is the Universal Time, converted to radians. S_T is the total W05 Poynting flux flowing into the Northern and Southern hemispheres, that is calculated using measured values of the IMF and solar wind velocity.

Results

Given a set of input parameters, a temperature is calculated for each of the 1620 grid cells, as shown in the example in Figure 2a, with local noon at 0 longitude. To obtain a higher resolution, or the temperature at any specified latitude/local time, a triangular interpolation of the gridded temperature values is used, as shown in Figure 2b.

Figure 3 shows the effects of varying the Universal Time, at a heating level of 200 GW. At 9 UT the peak temperature is found in the southern hemisphere, while at 21 UT the peak is in the northern

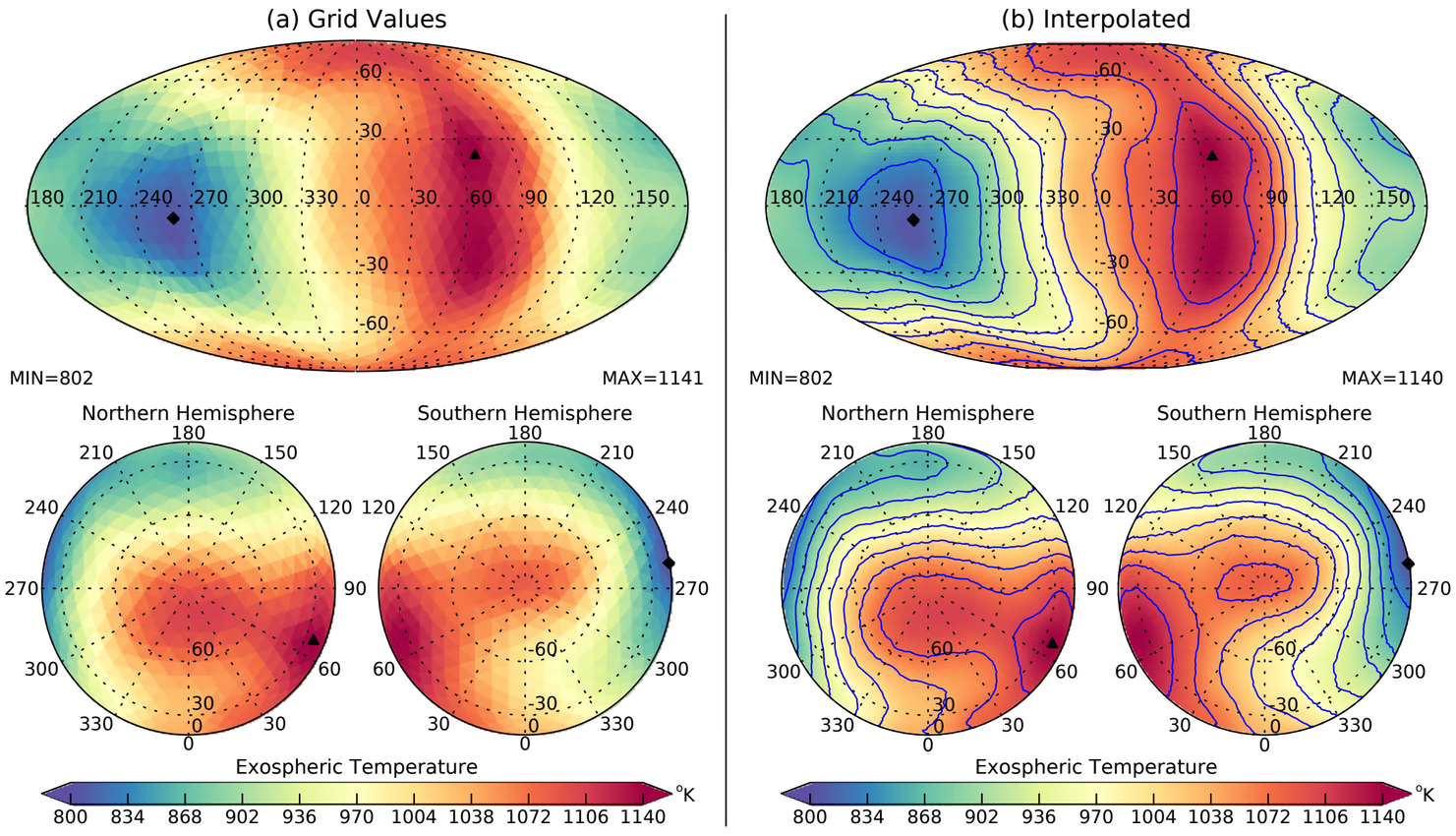

Figure 2. Example map of exospheric temperature variations calculated with ΔT=100°K, day of year=80, UT=15 h, both S_{10} and M_{10}=120 sfu, and polar heating is 50 GW in both hemispheres. (a) Shows the values in each grid cell, and (b) shows results using a triangulated interpolation.

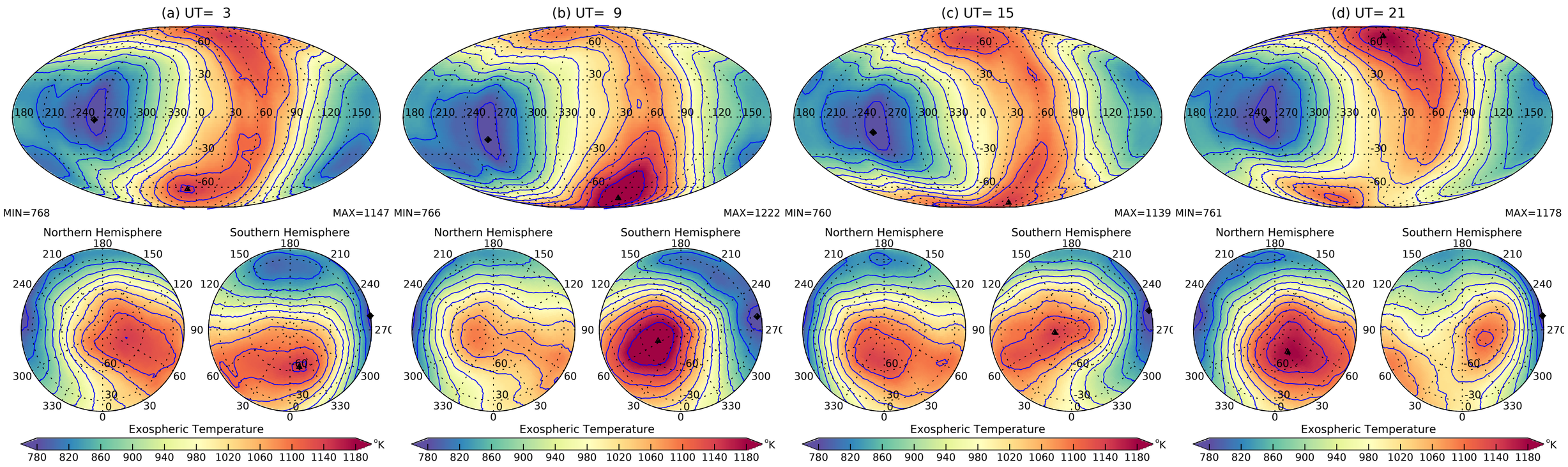

Figure 3. Examples showing influence of Universal Time on the maps of exospheric temperature. In (a)–(d) the UT is set to 3, 9, 15, and 21 hours, while the other parameters are fixed: ΔT=100K, day of year=80, both S_{10} and M_{10}=120 sfu, and the polar energy flux is 200 GW in both hemispheres.

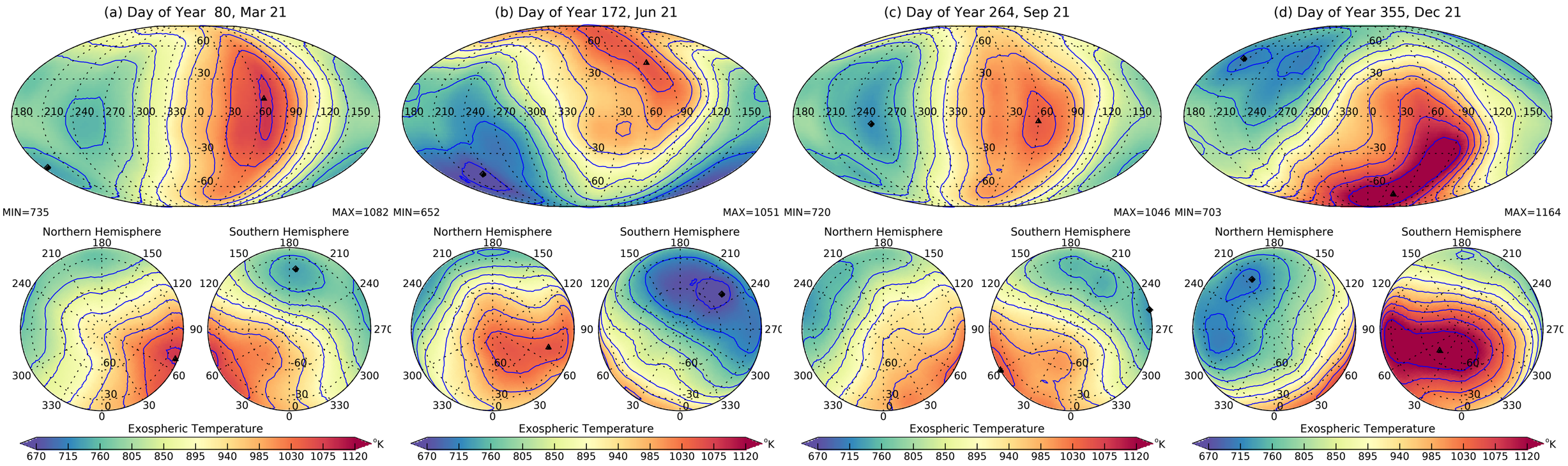

Figure 4. Maps of exospheric temperatures with only the day-of-year changed (equinox and solstice dates), while the other parameters are fixed: ΔT and the polar energy flux are set to zero, UT=3 h, both S_{10} and M_{10}=120 sfu.

hemisphere, due to the rotation of the magnetic poles around the geographic pole. The day-of-year also has a significant effect, as shown in Figure 4 for days 80, 172, 264, and 355 (equinox and solstice).

Figures 5 and 6 show graphs of exospheric temperatures from the model (red lines) on 26—28 July 2004, with dashed lines indicating global minimum/maximum temperatures. Blue lines show the values derived from the GRACE A and CHAMP measurements. For comparison, the

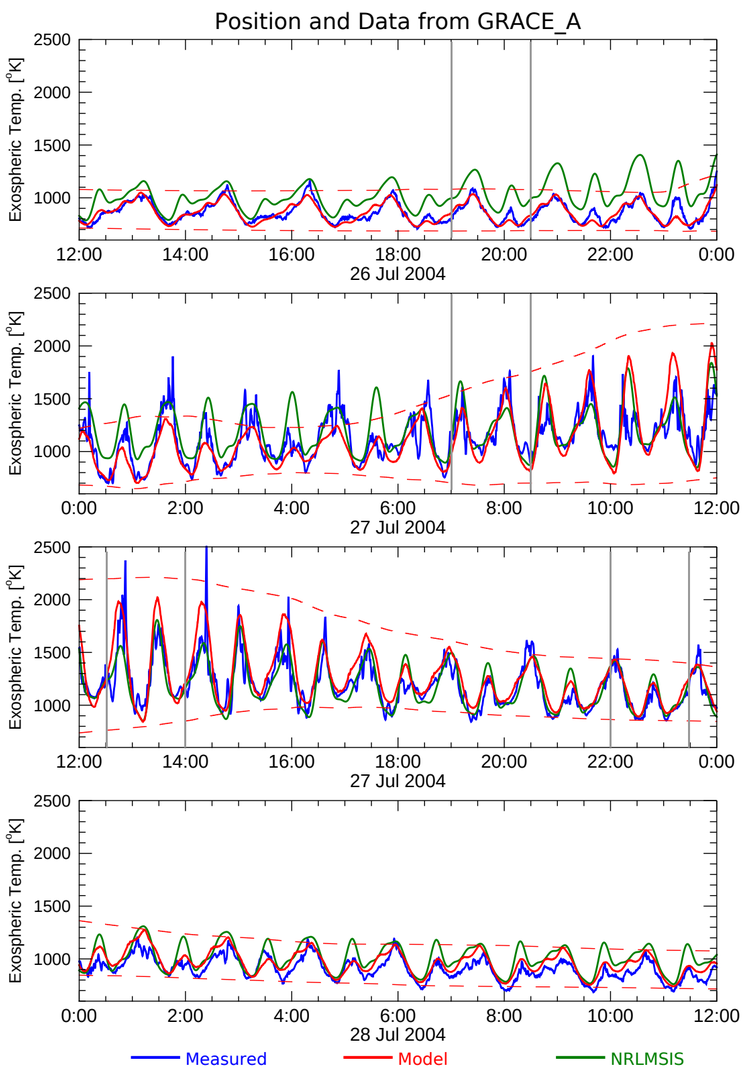

Figure 5. Exospheric temperatures along the GRACE A orbit, from 12 UT, 26 July to 12 UT, 28 July, 2004.

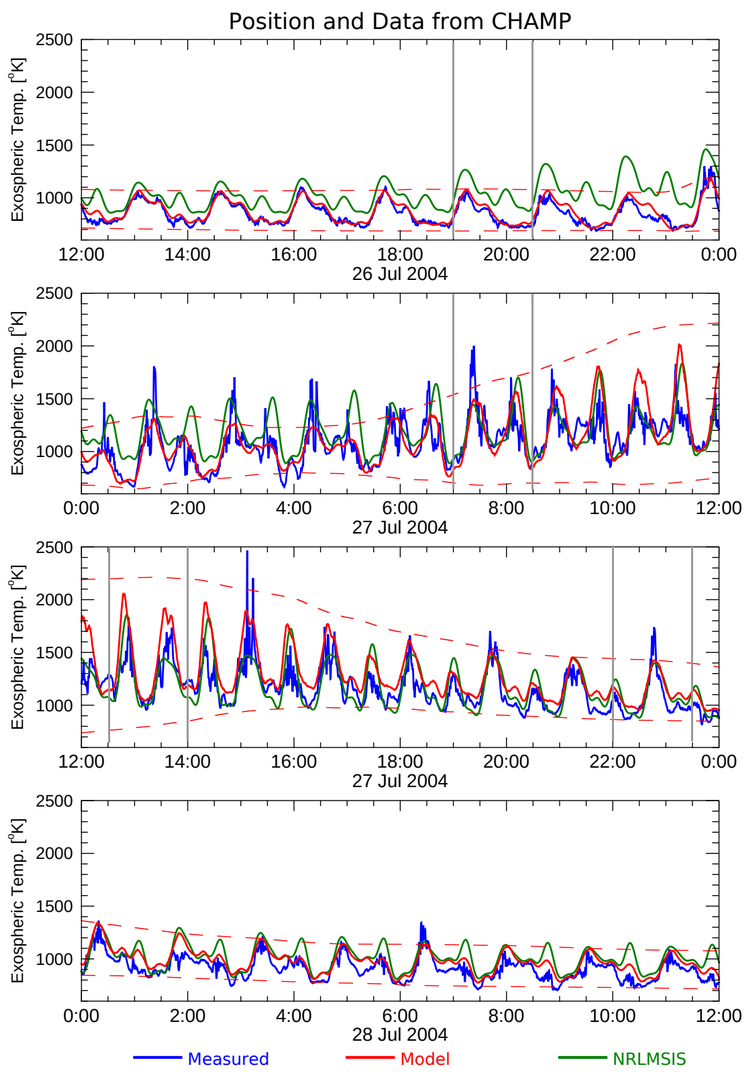

Figure 6. Exospheric temperatures along the CHAMP orbit, from 12 UT, 26 July to 12 UT, 28 July, 2004.

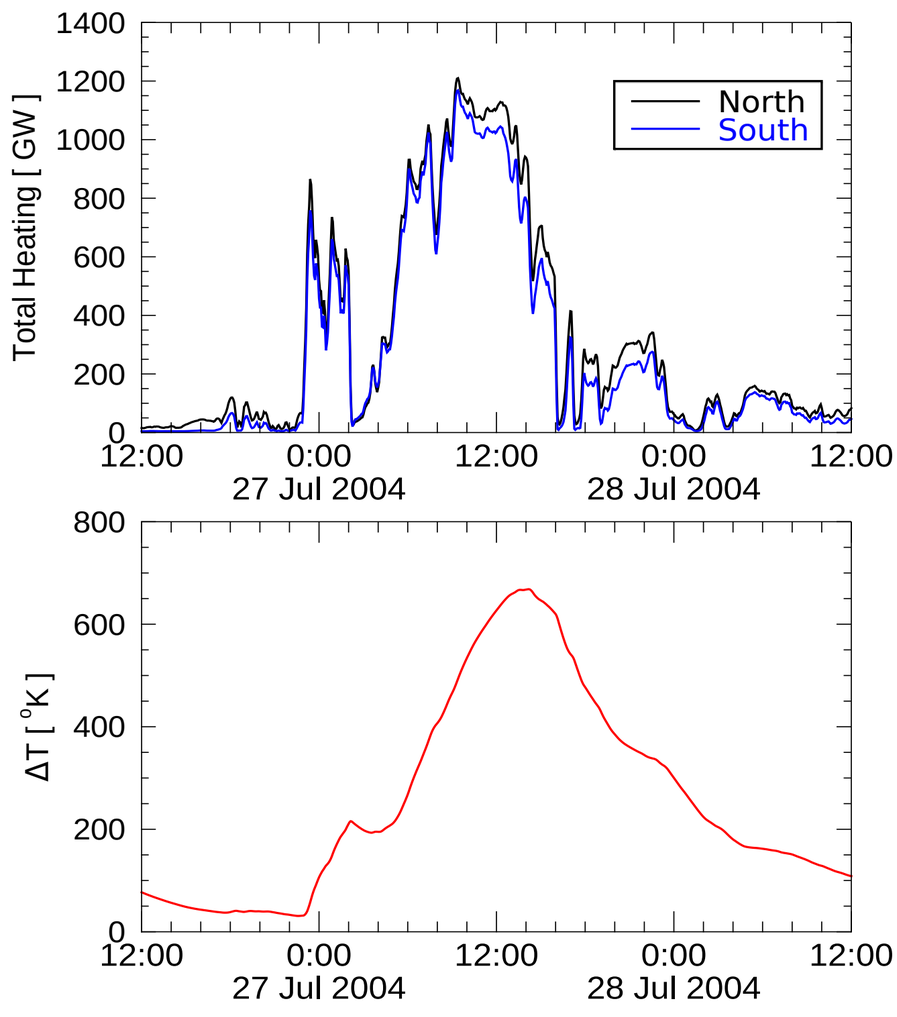

Figure 7. Total Poynting flux in Northern and Southern hemispheres, from 12 UT, 26 July to 12 UT, 28 July, 2004, and the derived ΔT temperature.

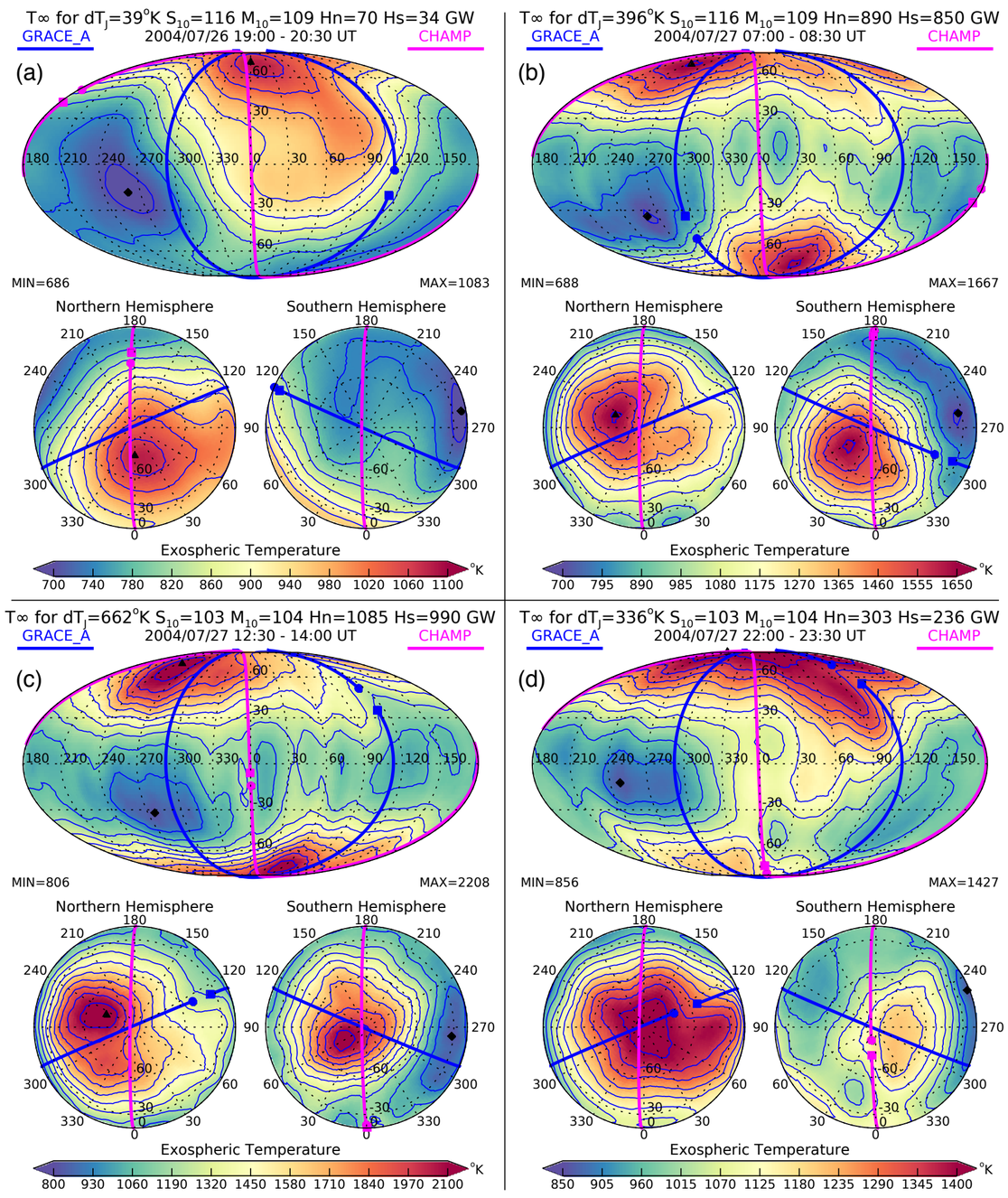

Figure 8. Maps of exospheric temperatures and GRACE A and CHAMP orbit tracks, 26–27 July 2004.

temperatures calculated by the NRLMSISE-00 model are shown with the green lines. Figure 7 shows the total Poynting flux and ΔT during this time period. Maps of the global temperatures and orbital tracks are shown in Figure 8, at the times indicated by the light gray lines in Figures 5 and 6.

Global values of the neutral densities are obtained by inserting these temperatures into the NRLMSISE-00 model, while retaining the original composition and other conditions at the low-altitude boundary at 120 km. Figures 9 and 10 show the densities that are derived for the same time period in July 2004 that was shown in Figures 5 and 6. The densities computed from the unmodified NRLMSISE-00 and JB2008 [*Bowman et al.,* 2008] models are shown for comparison. Figures 11 and 12 show densities computed for the major storm interval on 20—21 November 2003, and improved predictions using the EXTEMPLAR method are evident.

The mean errors and standard deviations of the density predictions were calculated for all CHAMP and GRACE data in 2002 through 2010. Comparing the model errors on a day-by-day basis, EXTEMPLAR had better scores than NRLMSISE-00 on ~83% of the days. Repeating the comparison with the JB2008 model, EXTEMPLAR had better scores on ~79% of the days. Improvements to the EXTEMPLAR method may be possible in the future, leading to better predictions of satellite drag and orbits. One upgrade that could be done is to introduce time delays that are computed separately for each grid cell.

Acknowledgments

DRW is supported by NASA grant NNX17AC04G to Virginia Tech, with additional support from a subcontract to Hampton University, on NASA grant NNX15AE05G.

References

Bowman, B. R., W. K. Tobiska, F. A. Marcos, C. Y. Huang, C. S. Lin, and W. J. Burke, A new empirical thermospheric density model JB2008 using new solar and geomagnetic indices, In AIAA 2008-6438, AIAA Astrodynamics Conference, Honolulu, HI, 2008.

Picone, J., A. Hedin, D. Drob, and A. Aikin, NRLMSISE-00 empirical model of the atmosphere: Statistical comparisons and scientific issues, *J. Geophys. Res., 107*(A12), 2002.

Tobiska, W. K., S. D. Bouwer, and B. R. Bowman, The development of new solar indices for use in thermospheric density modeling, *J. Atmos. Sol. Terr. Phys., 70,* 803, 2008.

Weimer, D. R., Improved ionospheric electrodynamic models and application to calculating Joule heating rates, *J. Geophys. Res., 110*, 2005.

Weimer, D. R., Predicting surface geomagnetic variations using ionospheric electrodynamic models, J*. Geophys. Res., 110*, 2005.

Weimer, D. R., B. R. Bowman, E. K. Sutton, and W. K. Tobiska, Predicting global average thermospheric temperature changes resulting from auroral heating, *J. Geophys. Res., 116*, 2011.

Weimer, D. R., M. G. Mlynczak, L. A. Hunt, and W. K. Tobiska, High correlations between temperature and nitric oxide in the thermosphere, *J. Geophys. Res.,120,* 1–12, 2015.

Weimer, D. R., M. G. Mlynczak, and L. A. Hunt, Intercalibration of neutral density measurements for mapping the thermosphere, *J. Geophys. Res., 121,* 5975–5990, 2016.

Weimer, D. R., M. G. Mlynczak, L. A. Hunt, and W. K. Tobiska, High correlations between temperature and nitric oxide in the thermosphere, *J. Geophys. Res.,120,* 1–12, 2015.

Weimer, D. R., P. M. Mehta, W. K. Tobiska, E. Doornbos, M. G. Mlynczak, D. P. Drob, J. T. Emmert, Improving neutral density predictions using exospheric temperatures calculated on a geodesic, polyhedral grid, submitted to *Space Weather*, 2019.

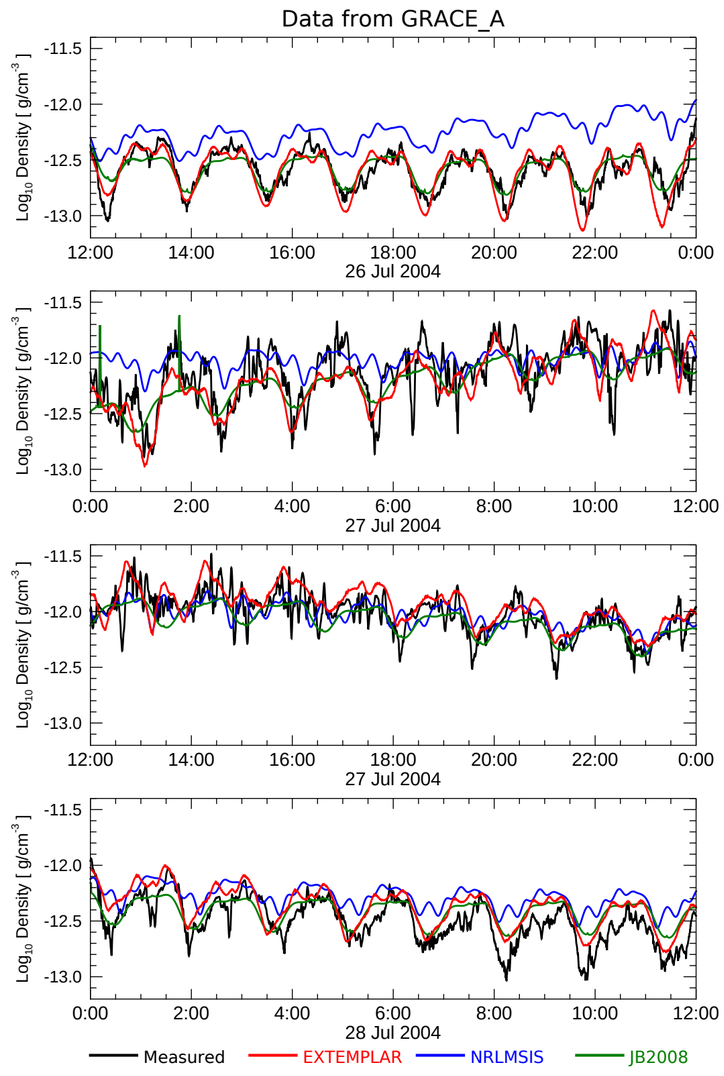

Figure 9. Neutral densities along the GRACE A orbit, from 12 UT, 26 July to 12 UT, 28 July, 2004.

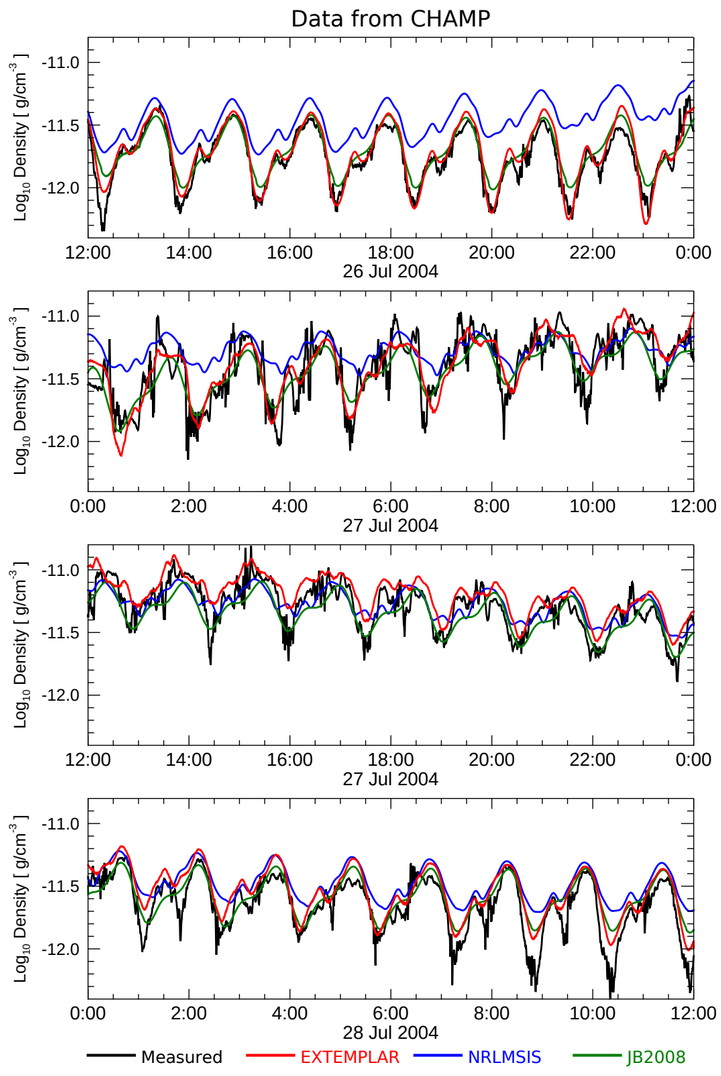

Figure 10. Neutral densities along the CHAMP orbit, from 12 UT, 26 July to 12 UT, 28 July, 2004.

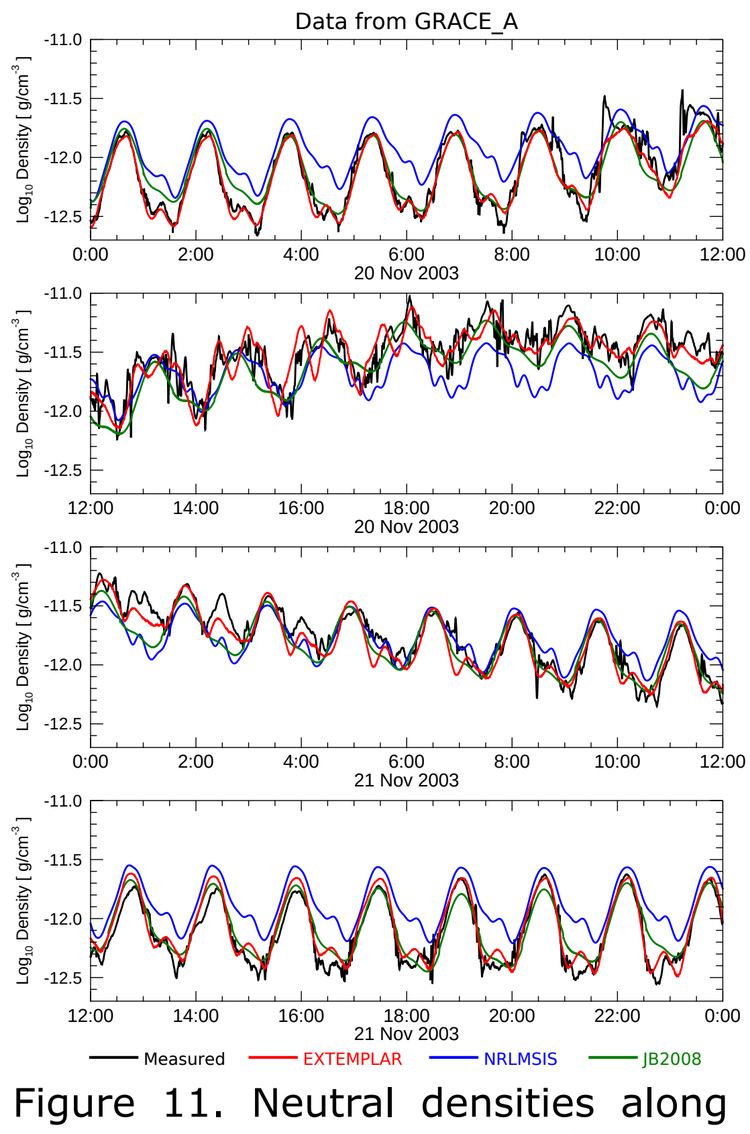

Figure 11. Neutral densities along the GRACE A orbit, 20—21 November 2003.

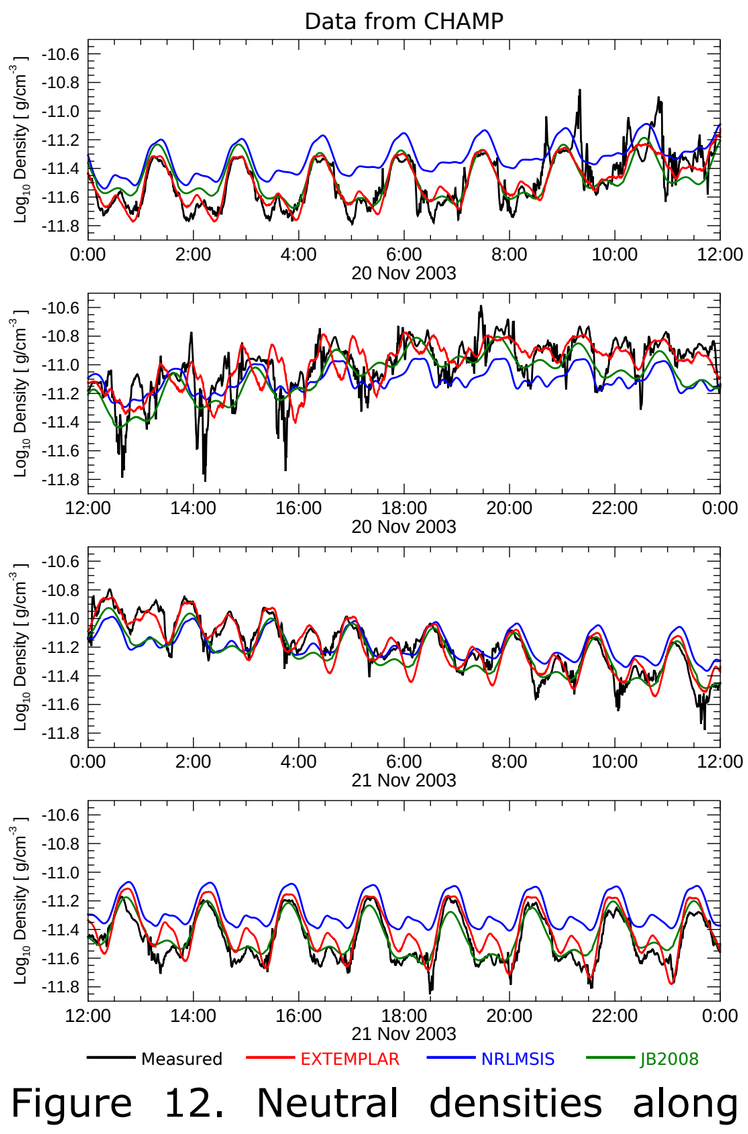

Figure 12. Neutral densities along the CHAMP orbit, 20—21 November 2003.